ISSN (Print) 1226-1750
ISSN (Online) 2233-6656
Journal of Magnetics 27(3), 233-237 (2022) https://doi.org/10.4283/JMAG.2022.27.3.233

A First-principles Study on Half-metallicity of LiCrSb/InSb Hybrid System

T. Thuy Hoang, S. H. Rhim*, and S. C. Hong*

Department of Physics and Energy Harvest Storage Research Center, University of Ulsan, Ulsan 44610, Republic of Korea

(Received 26 June 2022, Received in final form 1 July 2022, Accepted 5 July 2022)

It was recently predicted that alkali-metal-based half-Heusler compounds have robust half-metallicity with wide band gaps (1.60-2.38 eV), and the half-metallicity is retained at surface and under severe strain. In this study, we investigate the half-metallicity and electronic structure of the LiCrSb/InSb hybrid system to reveal real applicability of an alkali-metal-based half-Heusler compound to spintronics using first-principles calculations. Half-metallicity at the interface is well retained, and a proximate effect opens a gap in the minority spin band of the InSb layer with band gaps of 0.55-0.65 eV. The whole LiCrSb/InSb hybrid system prefers magnetization parallel to the plane.

Keywords : half-metals, half-Heusler, spintronics, wide band gap, first-principles calculation

1. Introduction

High degree of spin-polarized current is essential in achieving a highly efficient spintronic device [1, 2]. A half-metal (HM), of which one spin channel is insulating, and the other spin channel is metallic, could realize 100 % spin-polarized current [3, 4]. Intensive works have been done to find HMs and have suggested some HM materials theoretically [5-12]. Some of them have been confirmed in experiments to have half-metallicity [13-16]. However, most of the predicted HMs have failed to retain their half-metallicities in real environments such as at room temperature, surface, or interface [17-19].

A recent first-principles study predicted that some alkali-metal-based half-Heusler compounds XCrZ (X = Li, Na, and K; Z = P, As, and Sb) exhibit robust half-metallicity with wide band gaps (1.60-2.38 eV) [20]. The half-metallicity is so robust to be retained under severe strain and at surface. Most of XCrZ are stabilized in the β-phase, unlike transition-element-based ones, which are stable in the α-phase. The band gap formation mechanism of XCrZ is identical to that of zinc-blende CrZ in principle since the CrZ sublattice of the β-phase XCrZ forms the zinc-blende structure. The alkaline element X expands the lattice constant, retaining structural stability. The expanded lattice constant is the main reason for the wide band gap of the alkaline-element-based half-Heusler compounds. In conclusion, they proposed LiCrAs, LiCrSb, NaCrAs, and NarCrSb to be the most feasible compounds in realizing practical applications to spintronics in terms of robustness of half-metallicity and good lattice mismatches with a typical semiconductor of InSb.

In this study, we investigate the electronic structure of LiCrSb/InSb hybrid system to reveal the feasibility of application of an alkaline-element-based half-Heusler compound to spintronics using a first-principles calculational method. The calculated lattice constant (6.42 Å) of LiCrSb is not only quite well matched with that (6.48 Å) of InSb [21], but also pretty good interface formation is expected since the element Sb is a common component of the LiCrSb and InSb compounds. Atomic structure, electronic structure, half metallicity, and magnetocrystalline anisotropy will be discussed with a focus on the LiCrSb/InSb interface.

2. Structural Models and Computational Methodology

To investigate electronic structure at the interface between LiCrSb and InSb, a symmetric slab model is composed of 21 layers in total with Sb terminated (001) surfaces at both ends of the slab, as shown in Fig. 1. The two-dimensional lattice constant is set to the same as

*Co-corresponding author: Tel: +82-52-259-2325
e-mail: sonny@ulsan.ac.kr
Tel: +82-52-259-2331, e-mail: schong@ulsan.ac.kr

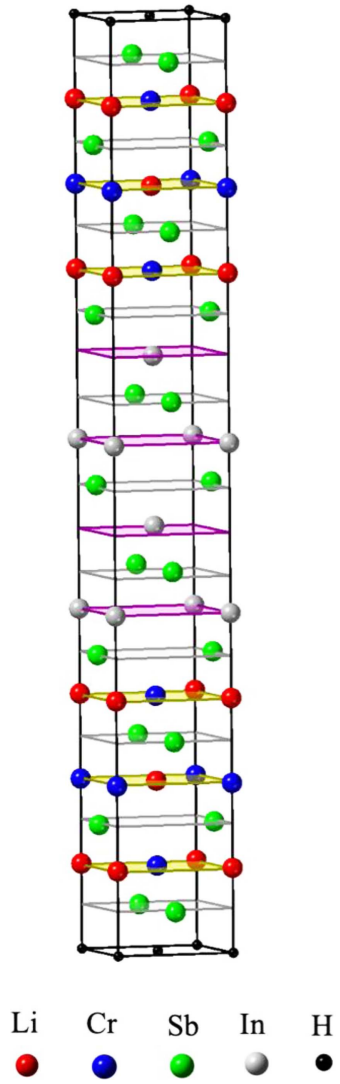

Fig. 1. (Color online) The 21-layer slab to simulate LiCrSb/InSb hybrid system with Sb terminated (001) surfaces. The Sb terminated (001) surfaces are passivated with hydrogen atoms. Red, blue, green, gray, and black spheres represent Li, Cr, Sb, In, and H.

InSb. The common Sb element of LiCrSb and InSb is positioned at the interface. The Sb terminated (001) surfaces are passivated with hydrogen atoms to minimize the effect of the surface on the electronic structure of the LiCrSb/InSb interface. A 15 Å vacuum is adopted between adjacent slabs to remove any spurious interactions. The lattice constant along the c-axis is determined from total energy calculations (optimized from total energy calculations).

The density-functional theory (DFT) calculations are carried out using the Vienna *ab initio* simulation package (VASP) [22], implementing the projector augmented-wave (PAW) pseudopotential method [23]. The exchange-correlation interactions between electrons are treated with the generalized gradient approximation (GGA) formulated by Perdew, Burke, and Ernzerhof (PBE) [24]. We use an energy cut-off of 550 eV for plane-wave-basis set and Monkhorst–Pack *k*-point meshes of 21 × 21 × 1 for Brillouin zone integration. The interlayer distances are relaxed until the force is less than 1×10^{-3} eV/Å. Total energy method is employed to estimate MCA energy, which can be expressed as $E_{MCA} = E_{\parallel} - E_{\perp}$, where $E_{\parallel}$ and $E_{\perp}$ are the total energies when the magnetization directions are parallel and perpendicular to the plane. To obtain reliable values of MCA, the Gaussian smearing method with small smearing of 0.05 eV and dense Monkhorst–Pack *k*-point meshes of 29 × 29 × 1 is adopted for the noncollinear calculations. The convergence of our calculations with respect to cut-off energy and the number of *k*-points are carefully checked.

3. Results and Discussion

3.1. Structural property

In this study, β-phase LiCrSb and zinc-blende InSb are taken into account. Since the sublattice of CrSb of the β-phase LiCrSb is the zinc-blende structure, the LiCrSb/InSb interface is established by sharing Sb as shown in Fig. 1. Two terminations of the LiCrSb surface are possible, LiCr-terminated and Sb-terminated. A previous study predicted that the LiCr-terminated surface does not retain the half-metallicity, while the Sb-terminated surface keeps the half-metallicity [20]. The broken half-metallicity of the LiCr-terminated surface will be remedied by a forming interface with the Sb element of InSb. Reflecting this prediction, the Sb-terminated surfaces are employed and passivated by hydrogen atoms (see Fig. 1).

The interlayer spacings are fully relaxed, whose values are listed in Table 1. For comparison, the interlayer spacings of strained LiCrSb (whose 2-dimensional lattice

Table 1. The interlayer distance (in Å) of LiCrSb/InSb hybrid system after being relaxed. The subscript n indicates the n-th layer from the surface. For example, d_{12} is the interlayer spacing between the surface and the subsurface layers.

	Interlayer distance
d_{12}	1.29
d_{23}	1.53
d_{34}	1.51
d_{45}	1.51
d_{56}	1.47
d_{67}	1.41
d_{78}	1.67

is the same as InSb) and InSb in bulk are also presented. The subscript number n in Table 1 denotes the n-th layer from the top surface of Fig. 1, i.e., the surface and the subsurface layers are denoted as 1 and 2, and the interface LiCr, Sb, and In layers are done as 6, 7, and 8, respectively. Under surface passivation by hydrogen, the interlayer spacing of LiCrSb quickly converges to about 1.51 Å. This is a little bit smaller than 1.59 Å of the strained LiCrSb. The smaller interlayer spacing is attributed to the surface tension. A 14-layer slab of LiCrSb with the same 2-dimensional lattice constant has further smaller interlayer spacing of 1.43 Å at the center of the slab [20].

Interlayer spacings of d_{67} (LiCr-Sb) and d_{78} (In-Sb) at the very interface are 1.41 Å and 1.67 Å, which are shrank and expanded compared to their bulk values of 1.59 and 1.62 Å, respectively. At this moment, we do not have any sophisticated answer to the reason. The spacing of the inner layers of InSb shows some oscillation. It implies that the film in the present study is not thick enough to reproduce the InSb bulk.

3.2. Magnetic property

The magnetic moments at the Cr, Sb, and In elements are listed in Table 2. As expected, the magnetic moment of the LiCrSb/InSb hybrid system comes mainly from the transition element Cr, while the elements of Sb and In have just induced magnetic moments as a proximate effect by the Cr element. The magnetic moment of the alkali-element Li and the inner layer In is too small to be listed in Table 2.

The magnetic moment of a half-metal is estimated by the Slater–Pauling rules [3]. For the present system, so-called “rule of 8” is applied. The rule is also valid to a zinc-blende-based system [25]. The magnetic moment per formula unit is given by $m_{tot} = (Z_t - 8)\ \mu_B$, where Z_t is the total number of valence electrons according to the rule. The rule may be understood with covalent bonding mechanism and the Hund’s first rule. In a zinc-blende material, 8 valence electrons per formula unit participate a covalent bonding. Half of the 8 electrons should be in spin-up states, and the rest half in spin-down states. The extra valence electrons, excluding the 8 electrons, occupy one spin direction state for the energy gain by the Hund's first rule so that the material becomes a half-metal with an integer magnetic moment per formula unit in unit of μ_B.

Table 2. Magnetic moments (in μ_B) of Sb, Cr, and In atoms in LiCrSb/InSb hybrid system. The number n in parenthesis indicates the n-th layer from the surface.

	m_s		m_s
Sb(1)	−0.32	Cr(2)	3.21
Sb(3)	−0.17	Cr(4)	3.70
Sb(5)	−0.16	Cr(6)	3.66
Sb(7)	−0.09	In(8)	0.05
Sb(9)	0.00	In(10)	0.00
Sb(11)	0.00		

As a result, the LiCrSb, CrSb, and InSb compounds have magnetic moments of 4.00, 3.00, and 0.00 μ_B per formula unit. The present LiCrSb/InSb hybrid slab has 25.0 μ_B in total. This value of magnetic moment is understood by the components of the present slab, which is consisted of 6 LiCr, 4 In, and 11 Sb layers. One extra Sb layer, compared to the counterparts for the covalent bonding, provides one more μ_B than magnetic moment of the 6 formula units of LiCrSb.

As seen in Table 2, the magnetic moment of Cr near the surface is reduced compared to the value in bulk, while the induced magnetic moment of Sb is enhanced in magnitude. The magnetic moments quickly converge to the strained bulk-like values (3.66 μ_B of Cr and 0.14 μ_B of Sb) [20], which again implies good passivation by the hydrogen atoms. The Sb atom of InSb has a positive magnetic moment of 0.05 μ_B just at the interface, while the rest Sb atoms of InSb do not show any magnetic moment like in bulk.

3.3. Electronic structure and half-metallicity

Layer-by-layer density of states (DOS) of the LiCrSb/InSb hybrid slab are presented in Fig. 2. Minority band gaps are clearly seen. The number in parenthesis denotes the order of a layer from the topmost surface layer. For example, (1) represents the very surface layer, (2) the subsurface, (3) the third layer from the surface, et cetera. The band gap of 1.10 eV at the surface is exactly the same as the Sb-terminated LiCrSb surface without the hydrogen passivation [20]. The band gap of the inner layer LiCrSb is 1.30 eV, which is much narrower than 1.58 eV of the center of non-passivated 14-layer LiCrSb slab [20]. The results imply that the 14-layer slab is thick enough to simulate a bulk surface, while the 6- or 7-layer slab is not. The interface LiCrSb has a band gap of 1.15 eV, which is a little bit wider than 1.10 eV at the surface, but much narrowed compared to 1.30 eV of the inner LiCrSb.

One interesting result of this LiCrSb/InSb hybrid system is that the InSb layer shows half-metallicity even though bulk InSb is a conventional semiconductor with a very narrow band gap of 0.235 eV [26]. The InSb layers have band gaps of 0.55-0.65 eV in the minority spin state, while it behaves like a metal in the majority spin state,

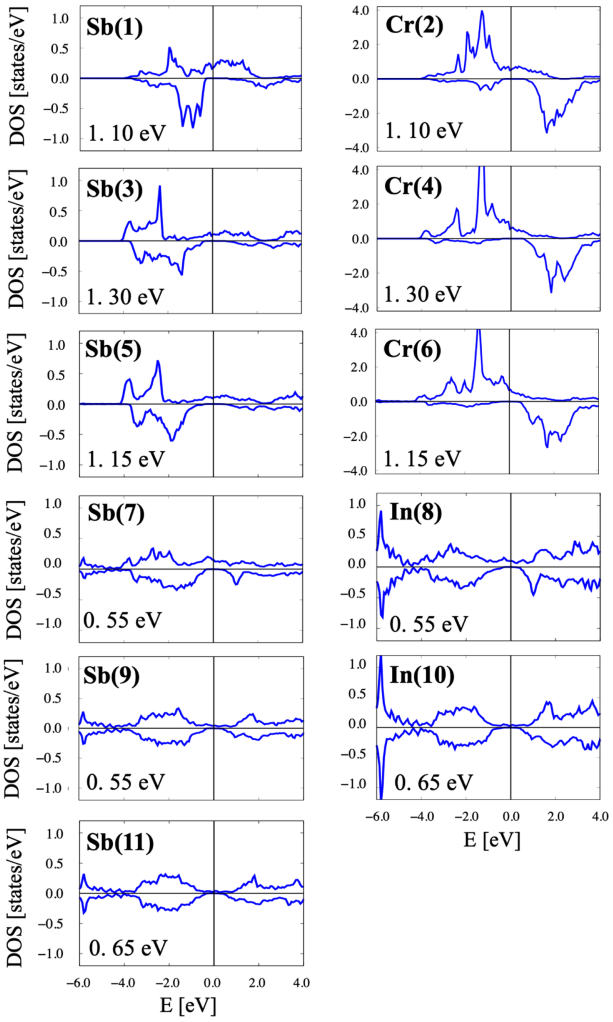

Fig. 2. (Color online) Layer-by-layer density of states (DOS) and minority spin band gaps of LiCrSb/InSb hybrid system. The number n in parenthesis indicates the n-th layer from the surface and the numerical energy value inside the figure box is the energy gap of the layer.

i.e., it has no band gap at the Fermi level. The interface InSb layer has quite similar DOS at the Fermi level to the interface LiCrSb, while the innermost InSb layer has almost zero DOS at the Fermi level. Hence, the half-metallicity of the InSb layer is a sort of a proximate effect. Of course, it is expected naturally that the innermost InSb layer shows a semiconducting behavior if the thickness of InSb layer increases. An interesting exploration would be what is the thinnest film to show a semiconducting behavior and what thickness is required for the innermost InSb layer to recover the bulk semiconducting behavior. These are out of the scope of the current study, and we leave these to future studies.

3.4. Magnetocrystalline anisotropy

Table 3. Layer-by-layer contributions to E_{MCA} (in meV/atom). The number n in parenthesis indicates the n-th layer from the surface.

	E_{MCA}
Sb(1)	0.16
Cr(2)	–0.19
Sb(3)	–0.60
Cr(4)	0.01
Sb(5)	0.02
Cr(6)	0.08
Sb(7)	–0.27
In(8)	0.06
Sb(9)	0.04
In(10)	0.00
Sb(11)	0.00

Perpendicular magnetocrystalline anisotropy (MCA) has an advantage in practical device applications [27-29]. Hence, MCA of the LiCrSb/InSb hybrid system has been investigated. The MCA energy is defined as:

$$E_{MCA} = E_{\parallel} - E_{\perp}$$

where $E_{\parallel}$ and $E_{\perp}$ are total energies for the magnetization directions, parallel and perpendicular to the plane.

The calculated E_{MCA} of the LiCrSb/InSb hybrid system is -1.22 meV in total, which implies that the easy magnetic axis is on the plane. For a detailed discussion, layer-by-layer contributions to E_{MCA} are listed in Table 3. Here, the contribution from Li is not listed since the contribution is negligible. Firstly, it is interesting that the non-magnetic element Sb contributes more than the magnetic element Cr. Secondly, the surface Sb layer contributes positively with the magnitude of 0.16 meV/atom. The value of 0.16 meV/atom is considerable noting that E_{MCA} of hcp Co in bulk is 0.015 meV/atom [30]. Thirdly, the contribution from each layer is quite different even though the element is the same. The contributions from Sb(1), Sb(3), Sb(5), and Sb(7) are 0.16, -0.60, 0.02, and -0.27 meV/atom, and those from Cr(2), Cr(4), and Cr(6) are -0.19, 0.01, and 0.08 meV/atom. We do not provide any answer to why this kind of behavior is shown, but quantum confinement may play a role.

4. Conclusion

We have done first-principles calculations on half-metallicity and electronic structure of LiCrSb/InSb hybrid system, focusing on the interface between LiCrSb and InSb. VASP is used with the implemented PAW method. To ensure the reliability of the calculations, an energy cut-off of 550 eV is taken for plane wave expansion of wave

function, and a Monkhorst–Pack *k*-point meshes of 21 × 21 × 1 is adopted for Brillouin zone integration. Half-metallicity at interface is predicted to be retained robustly. Proximate effect opens a gap in minority spin band of the InSb layer with band gaps of 0.55-0.65 eV interestingly. As a result, the whole LiCrSb/InSb hybrid system becomes half-metallic with a band gap of 0.55 eV. The LiCrSb/InSb hybrid system prefers parallel magnetization to the plane, but the Sb surface does perpendicular to the plane.

Acknowledgments

This work is supported by National Research Foundation of Korea funded by Ministry of Science and ICT (2016M3D1A1027830 and NRF-2019R1I1A3A01059880).

References

[1] Y. Lu, X. W. Li, G. Q. Gong, G. Xiao, A. Gupta, P. Lecoeur, J. Z. Sun, Y. Y. Wang, and V. P. Dravid, Phys. Rev. B **54**, R8357 (1996).
[2] E. Y. Tsymbal, O. N. Mryasov, and P. R. LeClair, J. Phys.: Condens. Matter **15**, R109 (2003).
[3] M. I. Katsnelson, V. Y. Irkhin, L. Chioncel, A. I. Lichtenstein, and R. A. de Groot, Rev. Mod. Phys. **80**, 315 (2008).
[4] R. A. de Groot, F. M. Mueller, P. G. van Engen, and K. H. J. Buschow, Phys. Rev. Lett. **50**, 2024 (1983).
[5] J. Ma, V. I. Hegde, K. Munira, Y. Xie, S. Keshavarz, D. T. Mildebrath, C. Wolverton, A. W. Ghosh, and W. H. Butler, Phys. Rev. B **95**, 024411 (2017).
[6] I. Galanakis, P. H. Dederichs, and N. Papanikolaou, Phys. Rev. B **66**, 174429 (2002).
[7] J. Deng, N. Liu, J. Guo, and X. Chen, Phys. Rev. B **99**, 184409 (2019).
[8] M. Baral and A. Chakrabarti, Phys. Rev. B **99**, 205136 (2019).
[9] L. Damewood, B. Busemeyer, M. Shaughnessy, C. Y. Fong, L. H. Yang, and C. Felser, Phys. Rev. B **91**, 064409 (2015).
[10] M. Rostami, M. Abedi, P. Amantorkaman, and F. Kanjouri, Vacuum **175**, 109278 (2020).
[11] R. L. Zhang, L. Damewood, Y. J. Zeng, H. Z. Xing, C. Y. Fong, L. H. Yang, R. W. Peng, and C. Felser, J. Appl. Phys. **122**, 013901 (2017).
[12] A. Dehghan and S. Davatolhag, J. Alloys Compd. **772**, 132 (2019).
[13] J. S. Parker, S. M. Watts, P. G. Ivanov, and P. Xiong, Phys. Rev. Lett. **88**, 196601 (2002).
[14] J. Y. T. Wei, N. C. Yeh, R. P. Vasquez, and A. Gupta, J. Appl. Phys. **83**, 7366 (1998).
[15] K. E. H. M. Hanssen, P. E. Mijnarends, L. P. L. M. Rabou, and K. H. J. Buschow, Phys. Rev. B **42**, 1533 (1990).
[16] R. J. Soulen, J. M. Byers, M. S. Osofsky, B. Nadgorny, T. Ambrose, S. F. Cheng, P. R. Broussard, C. T. Tanaka, J. Nowak, J. S. Moodera, A. Barry, and J. M. D. Coey, Science **282**, 85 (1998).
[17] Yu. S. Dedkov, M. Fonine, C. König, U. Rüdiger, and G. Güntherodt, Appl. Phys. Lett. **80**, 4181 (2002).
[18] M. Jourdan, E. A. Jorge, C. Herbort, M. Kallmayer, P. Klaer, and H.-J. Elmers, Appl. Phys. Lett. **95**, 172504 (2009).
[19] B. Varaprasad, A. Srinivasan, Y. Takahashi, M. Hayashi, A. Rajanikanth, and K. Hono, Acta Mater. **60**, 6257 (2012).
[20] T. Thuy Hoang, S. H. Rhim, and S. C. Hong, Phys. Rev. Mater. **6**, 055001 (2022).
[21] M. E. Straumanis and C. D. Kim, J. Appl. Phys. **36**, 3822 (1965).
[22] P. E. Blöchl, Phys. Rev. B **50**, 17953 (1994).
[23] G. Kresse and J. Furthmüller, Phys. Rev. B **54**, 11169 (1996).
[24] J. P. Perdew and Y. Wang, Phys. Rev. B **45**, 13244 (1992).
[25] I. Galanakis and P. Mavropoulos, Phys. Rev. B **67**, 104417 (2003).
[26] Z. M. Fang, K. Y. Ma, D. H. Jaw, R. M. Cohen, and G. B. Stringfellow, J. Appl. Phys. **67**, 7034 (1990).
[27] D. Weller and A. Moser, IEEE Trans. Magn. **35**, 4423 (1999).
[28] K. Yagami, A. A. Tulapurkar, A. Fukushima, and Y. Suzuki, Appl. Phys. Lett. **85**, 5634 (2004).
[29] Brahim Marfoua and Jisang Hong, J. Magn. **26**, 265 (2021).
[30] D. Weller, G. R. Harp, R. F. C. Farrow, A. Cebollada, and J. Sticht, Phys. Rev. Lett. **72**, 2097 (1994).